Acta Crystallographica Section D
Biological Crystallography
ISSN 0907-4449

Structural analysis of *Tityus serrulatus* Ts1 neurotoxin at atomic resolution: insights into interactions with Na^+ channels

Carlos Basílio Pinheiro,[a]† Sérgio Marangoni,[b] Marcos H. Toyama[b] and Igor Polikarpov[a,c]*

[a]Laboratório Nacional de Luz Síncrotron (LNLS), CP 6192, CEP 13084-971, Campinas/SP, Brazil, [b]Departamento de Bioquímica, Instituto de Biologia (UNICAMP), CP 6109, CEP 13083-970, Campinas/SP, Brazil, and [c]Grupo de Cristalografia, Departamento de Física em São Carlos, USP, Av. Trabalhador Saocarlense, 400 CEP 13560-970 São Carlos/SP, Brazil

† Present address: Institut de Cristallographie, Université de Lausanne BSP – Dorigny, CH-1015 Lausanne, Switzerland.

Correspondence e-mail: ipolikarpov@if.sc.usp.br

Received 3 September 2002
Accepted 18 November 2002

PDB Reference: neurotoxin Ts1, 1npi, r1npisf.

The structure of the Ts1 toxin from the Brazilian scorpion *Tityus serrulatus* was investigated at atomic resolution using X-ray crystallography. Several positively charged niches exist on the Ts1 molecular surface, two of which were found to coordinate phosphate ions present in the crystallization solution. One phosphate ion is bound to the conserved basic Lys1 residue at the Ts1 N-terminus and to residue Asn49. The second ion was found to be caged by residues Lys12, Trp54 and Arg56. Lys12 and Tyr/Trp54 residues are strictly conserved in all classical scorpion β-neurotoxins. The cavity formed by these residues may represent a special scaffold required for interaction between β-neurotoxins and sodium channels. The charge distribution on the Ts1 surface and the results of earlier chemical modification studies and side-directed mutagenesis experiments strongly indicate that the phosphate-ion positions mark plausible binding sites to the Na^+ channel. The existence of two distinct binding sites on the Ts1 molecular surface provides an explanation for the competition between Ts1, depressant (LqhIT2) and excitatory (AaHIT) neurotoxins.

1. Introduction

The long-chain Na^+-channel-specific scorpion toxins are generally composed of 61–76 amino-acid residues. Two major categories of these toxins (named α and β) have been classified according to their pharmacological and vertebrate channel-binding properties (Gordon *et al.*, 1998). The α-toxins inhibit or slow Na^+-channel inactivation in a voltage-dependent manner (Jover, Couraud *et al.*, 1980; Jover, Moutot-Martin *et al.*, 1980; Couraud *et al.*, 1982). The β-toxins shift the voltage dependence of Na^+-channel activation to more negative potentials, causing the membrane to fire spontaneously and repetitively, without influencing the inactivation (Couraud *et al.*, 1982; Meves *et al.*, 1984). Toxin II from *Androctonus australis* Hector (AaHII) and toxin II from *Centruroides suffusus suffusus* (CssII) are considered to be prototypes of the α- and β-neurotoxins, respectively. Competition with ^{125}I-AaHII and with ^{125}I-CssII in binding to sodium channels serves as a major tool for the classification of unknown scorpion toxins into the α- and β-classes (Gordon *et al.*, 1998). Typical α- and β-toxins bind to distinct sites on sodium channels and do not affect each other's binding properties (Gordon *et al.*, 1998). Furthermore, they show an unusual ability to discriminate between insect and mammalian sodium channels and their high affinity and specificity have led to their use as molecular probes to identify and characterize functional regions within sodium-channel subunits (Catterall, 1992; Gordon *et al.*, 1996).

Both α- and β-neurotoxins have been further subdivided into subgroups based on similarities in their three-dimensional

structures, species specificity and pharmacological effects (Possani *et al.*, 1999). In particular, anti-insect selective excitatory (Zlotkin *et al.*, 1978; Pelhate & Zlotkin, 1982; Zlotkin, 1993) and depressant excitatory (Zlotkin *et al.*, 1978, 1985; Zlotkin, 1993) toxins cause the same pharmacological effects as other β-toxins competing with them for the same receptor-binding site (Barhanin *et al.*, 1982; de Lima *et al.*, 1986; Gordon *et al.*, 1992; de Lima & Martin-Euclaire, 1995; Cestèle *et al.*, 1997; Froy *et al.*, 1998) and are therefore considered to be members of the β-neurotoxin family.

The amino-acid sequences of α- and β-neurotoxins show a variable degree of identity (Possani *et al.*, 1999). There are several strictly conserved residues in the primary structure of the long-chain neurotoxins, including eight cysteines forming the invariant disulfide bridges C15–C37, C23–C42, C27–C44 and C11–C61 (Fig. 1; all residues named according to the Ts1 numbering). Excitatory toxins are a remarkable exception to this rule. The link between the C-terminus and the core of the protein is not made *via* the highly conserved disulfide C61–C11, but instead *via* a C39–C61 disulfide bridge (Oren *et al.*, 1998).

A number of three-dimensional α and β scorpion-toxin structures determined both by X-ray diffraction techniques and NMR spectroscopy are available to date (Zhao *et al.*, 1992; Housset *et al.*, 1994; Li *et al.*, 1996; He *et al.*, 1999, 2000; Polikarpov *et al.*, 1999; Lee *et al.*, 1994; Jablonsky *et al.*, 1995, 1999; Landon *et al.*, 1996; Tugarinov *et al.*, 1997; Blanc *et al.*, 1997; Krimm *et al.*, 1999; Pintar *et al.*, 1999). All of them share a highly conserved dense core formed by a cysteine-stabilized α-helix/β-sheet (CS$\alpha\beta$) motif consisting of three or four antiparallel β-strands and an α-helix interlinked by two or three invariant disulfide bridges (Landon *et al.*, 1997). This motif is found in many proteins exhibiting antibiotic or toxic activity (Landon *et al.*, 1996). The insect-specific excitatory neurotoxin Bj-xtrIT possesses a second short α-helix at the C-terminus (Oren *et al.*, 1998), which is unique among the known long-chain Na^+-channel-specific scorpion toxins.

The structural basis of the long-chain neurotoxin binding specificity to the Na^+ channel is not yet completely understood. It has been suggested that one face of the neurotoxins, containing a number of conserved aromatic residues, is involved in Na^+-channel recognition (Fontecilla-Camps *et al.*, 1981). It has also been shown that chemical modification of the N-terminal residues Lys1 in Ts1 (Possani *et al.*, 1985), Arg1 in AaHI and AaHIII (el Ayeb *et al.*, 1986; Kharrat *et al.*, 1990), Val1 and Arg2 in AaHIII (Kharrat *et al.*, 1990) and the α-amino group in AaHI (Kharrat *et al.*, 1990) produces weakly active or inactive derivatives. Chemical modification of the basic residues Arg25 in CssII (el Ayeb *et al.*, 1986), Arg56 in AaHII (Kharrat *et al.*, 1990) and Arg60 in AaHI (Kharrat *et al.*, 1990) also results in a remarkable loss of activity. Cleavage of the six N-terminal residues of Ts1 or five N-terminal residues of BomIII gives non-toxic derivatives (Possani *et al.*, 1985; el Ayeb *et al.*, 1986). Chemical modification of the conserved Tyr residues in AaHIII and Trp39 in AaHII (Kharrat *et al.*, 1989) induced a remarkable loss of biological activity. Toxicity and binding-affinity tests have shown that residues Trp54 and Trp39 from the aromatic conserved cluster and Lys12 are important to Ts1 activity (Hassani *et al.*, 1999). The simultaneous chemical modification of Lys12, Trp54 and Trp39 reduced the apparent affinity of Ts1 for both insects and mammals by two orders of magnitude. Mutagenesis studies of the α-neurotoxin LqhαT show that the aromatic residues Tyr9 and Phe16 and the positively charged residues Lys8, Arg17, Lys60 and Arg62 may interact directly with putative recognition areas on the Na^+-channel receptor and are important in influencing its surface electrostatic potential (Zilberberg *et al.*, 1997). Mutagenesis studies and circular-dichroism spectroscopy on Bj-xtrIT (Froy *et al.*, 1998) suggested a possible recognition role played by its C-terminus and revealed the importance of Ile65 and Ile66 to protein toxicity.

Despite all the available structural and pharmacological data, the precise location of the

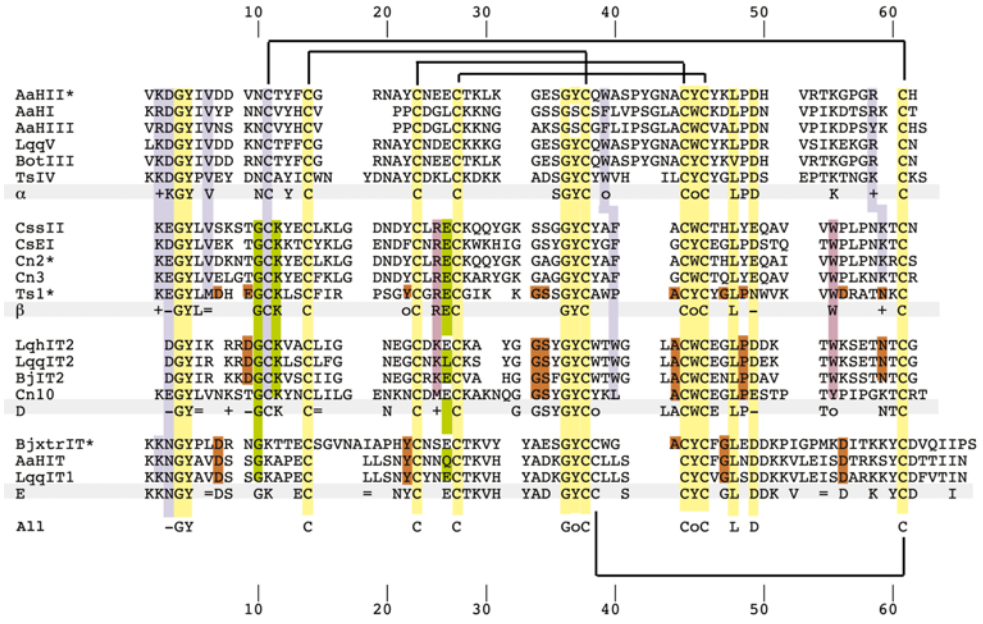

Figure 1
Classical α- and β-, depressant (D) and excitatory (E) toxin sequence alignment. The toxins marked with asterisks are of known three-dimensional structure. Columns coloured yellow, violet, green and pink indicated residues that are globally invariant, conserved in α/β/D, conserved in β/D/E and conserved in β/D toxins, respectively. Columns coloured red highlight additional residues common to Ts1 and D- or E-toxin amino-acid sequences. '+' represents positively charged residues, '−' negatively charged residues, '=' apolar residues and 'o' aromatic residues. Rows labelled α, β, D and E and All indicate the average sequences. The alignment was performed using the program *CLUSTALW* (Thompson *et al.*, 1994).

Table 1
Ts1 neurotoxin data-collection and data-reduction parameters.

Values in parentheses for the average $I/\sigma(I)$ and completeness refer to the last resolution shell (1.19–1.16 Å). Observed reflections (obs) have intensities $I \geq 2\sigma(I)$.

Data set	*A*	*B*
Data collection		
Diffractometer type	MAR	
Detector type	Imaging plate	
Scanning type	Oscillations	
$\Delta\varphi$/frame (°)	2.0	
Exposure mode	Dose	
Temperature (K)	298	
λ (Å)	1.28	1.38
Detector distance (mm)	73.2	74.0
Data reduction and integration		
Space group	*P*1	*P*1
Unit-cell parameters		
a (Å)	23.39 (4)	23.27 (4)
b (Å)	36.71 (3)	36.62 (4)
c (Å)	31.21 (1)	31.13 (2)
α (°)	90.00 (3)	89.98 (4)
β (°)	105.57 (7)	105.4 (1)
γ (°)	90.01 (3)	89.99 (3)
Volume ($\times10^{-3}$ Å^3)	25.81 (8)	25.6 (1)
Maximal resolution (Å)	1.16	1.25
Integrated reflections	28451	25388
Average $I/\sigma(I)$	11 (2)	12 (3)
Data reduction and scaling		
2θ range (°)	6.8–73.2	
Resolution range (Å)	1.16–12.0	
Space group	$P2_1$	
Unit-cell parameters		
a (Å)	23.25 (1)	
b (Å)	36.61 (4)	
c (Å)	31.10 (4)	
β (°)	105.58 (9)	
Volume ($\times10^{-3}$ Å^3)	25.50 (8)	
Unique reflections (all)	16095	
Unique reflections (obs)	11943	
R_{sym} (all)	0.078	
Completeness (%)	92 (52)	

binding/toxic sites of the scorpion neurotoxins has not yet been determined. The best that can be concluded at present is the general importance of the positively charged residues, of the conserved aromatic residues and of the structural regions such as the N- and C-termini for both α- and β-toxins. It is not defined whether there are general binding/toxic key residues in those toxins or if the binding-mechanism role is played by a combination of the three-dimensional arrangement, surface-charge distribution and the extension and mobility of the C-terminus.

The long-chain neurotoxin Ts1 (also know as Ts-γ and Ts VII) is the major component of the venom of the Brazilian scorpion *Tityus serrulatus* (Possani *et al.*, 1981). Ts1 has 61 amino-acid residues and is an active β-toxin, with one of the highest affinities known for both mammalian and insect sodium channels (K_d = 4.0–9.0 p*M*). Ts1 competes with the mammal-selective β-toxin *C. suffusus suffusus* (Barhanin *et al.*, 1982, 1984), with the excitatory insect-selective toxin from *A. australis* Hector (de Lima *et al.*, 1986) and with the depressant excitatory insect-selective toxin from *Leiurus quinquestriatus hebraeus* (Gordon *et al.*, 1992) in rat brain and cockroach nerve-cord synaptosomal preparations. These results indicate that Ts1 binds to homologous clusters of receptor sites on sodium channels in both insects and mammals, in contrast to the phylogenic selectivity common for the majority of the neurotoxins. This fact corroborates the concept that specificity in neurotoxins is related to the degree of toxicity (Selisko *et al.*, 1996).

The Ts1 room-temperature structure has been previously determined by X-ray crystallography at 1.7 Å resolution (Polikarpov *et al.*, 1999). This structure will subsequently be referred to as the high-resolution Ts1 model (Ts1-HR). In the present work, the first atomic resolution crystal structure of the highly toxic β-neurotoxin Ts1 (Ts1-AR) is described. X-ray diffraction experiments were performed on a crystal grown in the presence of potassium phosphate (Golubev *et al.*, 1998). The data collected at the synchrotron source extend to 1.16 Å resolution. Atomic resolution refinement allowed the determination of the individual atomic displacement parameters and the standard deviations (e.s.d.s) for each refined variable, as well as the refinement of the occupation parameters for special groups of atoms and water molecules. In addition to a number of disordered side chains and more than 100 water molecules, the C- and N-termini and two phosphate ions could be unambiguously identified in the electron-density maps. The charge distribution on the Ts1 surface and the results of the earlier chemical modification and side-directed mutagenesis studies strongly indicate that the phosphate-ion positions mark possible binding sites to the Na^+ channel. To the best of our knowledge, this is the first structural evidence of the exact locations of the two distinct putative receptor-binding sites in scorpion neurotoxins. Detailed analysis of these binding sites provides a plausible explanation of the binding competition between Ts1, excitatory and depressant toxins.

2. Materials and methods

2.1. Crystallization and data collection

A single crystal of the Ts1 protein (molecular weight 7.97 kDa) was grown by the hanging-drop vapour-diffusion method (Golubev *et al.*, 1998). The crystal grew in the monoclinic space group $P2_1$, with one toxin molecule in the asymmetric unit. Data were collected at the Protein Crystallography beamline of the Brazilian National Synchrotron Light Laboratory (LNLS; Polikarpov, Oliva *et al.*, 1998; Polikarpov, Perles *et al.*, 1998) from a single crystal mounted in a glass capillary. Data collection was performed at room temperature (298 K) using two wavelengths: 1.28 and 1.38 Å. The best resolution achieved with a 35 cm MAR Research imaging-plate detector was 1.16 Å. Image integration was performed using *DENZO* in space group *P*1. Scaling was performed using *SCALEPACK* (Otwinowski & Minor, 1993) in space group $P2_1$. The data sets measured at the two wavelengths were merged. At the refinement stage, it was found that inclusion of the estimated intensities of approximately 300 unique overloaded reflections in the data scaling improved the quality of the calculated electron-density map.

Therefore, these reflections were kept in the experimental diffraction data set. Final data-collection and data-reduction statistics are presented in Table 1.

2.2. Structure refinement

The Ts1-HR model (PDB code 1b7d) was initially adjusted to the electron-density map calculated from the data collected at 1.16 Å resolution. Significant differences between the Ts1-HR model and the density maps in both the backbone and side chains were corrected manually on a graphics workstation using the program *O* (Jones *et al.*, 1991). In order to avoid any structural bias, several cycles of simulated annealing from 1000 to 300 K were performed using the program *CNS* (Brünger *et al.*, 1998). Three different structural models obtained after the simulated-annealing procedure were used as the input in a standard macromolecular refinement. The Ts1-AR model refinement was performed with *SHELXL*97 (Sheldrick & Schneider, 1997). The function $wR(F)$[1] was refined using conjugate-gradient least-squares (CGLS) minimization (Konnert & Hendrickson, 1980). In order to calculated the standard deviations of the refined parameters, one final cycle of conventional unconstrained full-matrix least-squares (LS) refinement was performed. The x, y, z coordinates and the displacement tensor of each neurotoxin atom were refined subject to stereochemical restraints. The bulk solvent was modelled following Babinet's principle (Moews & Kretsinger, 1975). The refinement agreement parameters obtained for the best starting model subjected to isotropical B-factor refinement are $R[I \geq 2\sigma(I)] = 0.217$ for 11 898 unique reflections and $R_{\rm free}[I \geq 2\sigma(I)] = 0.244$ for 613 reflections randomly selected from native data and omitted during all the refinement cycles (Brünger, 1992). No crystallographic water molecules were included during this first refinement step. Anisotropic B-factor refinement was carried out as the next step. 48 water molecules with isotropic displacement tensors were included in the structural model. The side chains of residues Glu2, Lys12 and Ser20 were modelled in double conformation. At this point, some H atoms were included in the refinement according to the riding model (Johnson, 1970), with no increase in the number of refinement parameters. Owing to the high quality of the electron-density maps, three additional disordered side chains (Tyr45, Trp54, Asn59), 55 new water molecules and a second phosphate ion could be unambiguously assigned to the density peaks found in subsequent refinement cycles. There was no indication of structural disorder of any of the four existing disulfide bridges. At the very end, 11 water molecules and all the remaining riding H atoms were included in the model. All displacement parameters, except those describing H atoms, were refined anisotropically. Disordered side chains, phosphate ions and water occupancies were refined. Of the 114 refined water molecules, only nine showed an occupancy parameter smaller than 0.4 and all of them could be identified in the $2F_o - F_c$ map contoured at 1σ ($\sigma = 0.05$ e Å^{-3}). The residual $F_o - F_c$ map had no peaks above 0.24 e Å^{-3} ($\sim 5\sigma$s) and all attempts to introduce new water molecules failed. The difference between R and $R_{\rm free}$ was stable at around 0.05 during the entire refinement procedure (data not shown). Table 2 shows the final refinement statistics for both the Ts1-HR and Ts1-AR models.

[1] $wR(F) = \sum_j w_j |F_{oj}^2 - F_{cj}^2| / \sum_j F_{oj}^2$.

Table 2
Ts1-AR and Ts1-HR (Polikarpov *et al.*, 1999) final refinement statistics parameters.

$R_{\rm free}$ values were calculated in the last CGLS refinement cycle. Observed reflections (obs) have intensities $I \geq 2\sigma(I)$.

Model	1.7 Å	1.16 Å
Refinement program	*REFMAC*	*SHELXL*
Refinement strategy	CGLS	CGLS
No. of parameters	1932	5797
No. of restraints	—	7118
No. of protein atoms	479	509
No. of solvent atoms	65	114
No. of ion atoms	5	10
$\Delta\rho_{\rm max}$ (e Å^{-3})	—	0.24
$\Delta\rho_{\rm min}$ (e Å^{-3})	—	−0.36
Final R indices (all)		
No. of unique reflections	5149	16095
No. of reference reflections	670	785
R (working + reference set)	—	0.1033
R (working set)	0.178	0.0974
$R_{\rm free}$	0.238	0.1587
Final R indices (obs)		
No. of unique reflections	—	12566
No. of reference reflections	—	623
R (working + reference set)	—	0.0878
R (working set)	—	0.0821
$R_{\rm free}$	—	0.1391

3. Results

3.1. The Ts1-AR structural model

The fold of the polypeptide chain of Ts1 is similar to that

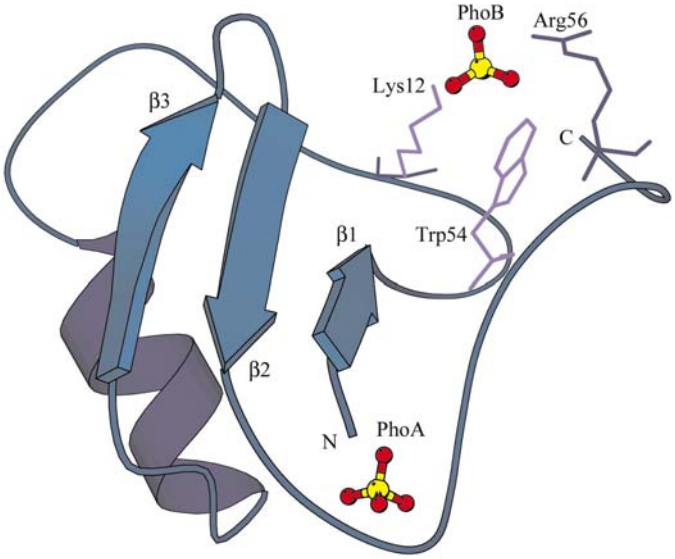

Figure 2
Ribbon representation of the 1.16 Å resolution refined model generated using *MOLSCRIPT* (Kraulis, 1991). The phosphate ion PhoA interacts with the N-terminal residues, whereas phosphate PhoB is bound to a Ts1 putative binding cavity formed by Lys12, Trp54 and Arg56. β, C and N represent β-strands, the C-terminus and the N-terminus, respectively.

seen in other long-chain toxins. A structural schematic view of the Ts1-AR model is given in Fig. 2 and the final refinement statistics are summarized in Table 2. The average B values ($B = 8\pi^2 U_{iso}$; U_{iso} is the isotropic displacement parameter) for the main-chain atoms, side-chain atoms and water molecules are 14 (1), 21 (4) and 34 (10) Å^2, respectively [average B values were calculated with the program *BAVERAGE* (Collaborative Computational Project, Number 4, 1994)]. The electron-density maps around the side chains of the residues Glu2, Lys12, Ser20, Tyr45, Trp54 and Asn59 clearly indicate multiple conformations. In contrast to the BmK M1 and BmK M4 structures (He *et al.*, 1999), no non-proline *cis*-peptide bonds were observed in the Ts1-AR structure. A detailed description of the Ts1 structural features relevant to recognition and binding to the Na^+ channel is presented below.

3.2. Conserved aromatic cluster

The Ts1 neurotoxin can be visualized as having two distinct triangular flat faces opposite to each other (Polikarpov *et al.*, 1999). One face contains the conserved aromatic cluster (Fontecilla-Camps *et al.*, 1981) formed by the residues Tyr4, Tyr36, Trp39, Tyr43, Tyr45 and Trp54. The side chains of Tyr4, which is strictly conserved in all long-chain neurotoxins, and of Tyr36 adopt an almost parallel orientation in the Ts1 structure. The aromatic ring of Tyr43 makes van der Waals contacts with the side chains of Tyr4 and Tyr36, being roughly perpendicular to both of them. Its hydroxyl group is also at a hydrogen-bonding distance from the carboxyl group of Glu2 in one of its conformers. In each of its two conformations, the Glu2 carboxyl group interacts differently with the hydroxyl group of Tyr43. In one of the conformers the distance from Glu2 OE2 to Tyr43 OH is 2.47 (4) Å, whereas in the second conformer the analogous distance is 2.78 (3) Å. It is interesting to note that the conformation of the Tyr43 side chain is maintained unperturbed despite the double conformation of Glu2. The relative orientation adopted by the side chains of residues Tyr4, Tyr36 and Tyr43 forms a 'herringbone' pattern, which is the spatial arrangement corresponding to the lowest energy for relatively solvent-exposed aromatic rings (Burley & Petsko, 1985).

The face opposite to the conserved aromatic cluster contains a number of positively charged residues: Arg18, Arg25, Lys30, Lys31 and Lys52. Most of these residues are exposed to the solvent. The side chains of residues Lys31 and Glu9 make crystal contacts with a symmetry-related Ts1 molecule. The side chains of residues Lys52 and Arg25 are the only ones with no clear electron density in the final difference maps.

3.3. The environment of the phosphate ions

The crystalline sample used in the present work was grown in a solution containing potassium phosphate at a concentration of approximately 50 mM (pH 6.0) (Golubev *et al.*, 1998). Considering the charge distribution at the Ts1 surface, it is reasonable to expect that the binding of negative ions would map the areas with the highest positive potential. Indeed,

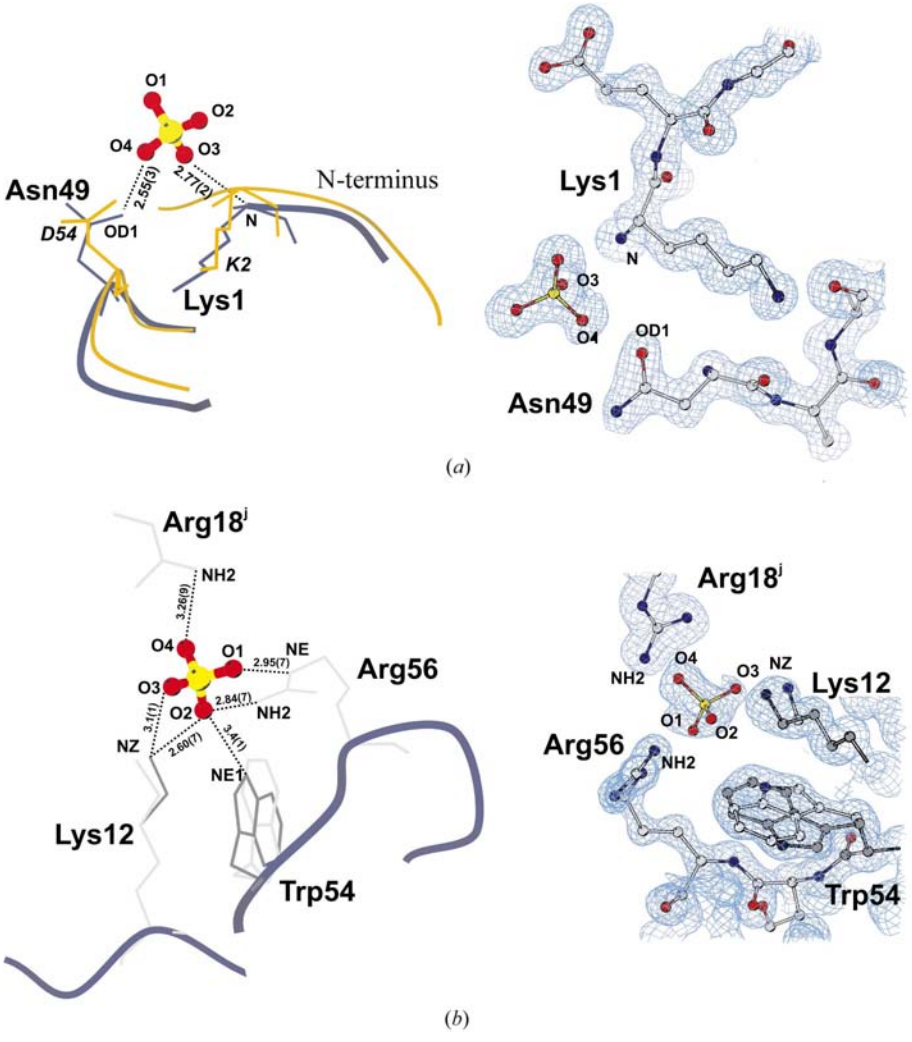

Figure 3
The structural environment of and the 1.16 Å resolution omit maps around the phosphate ions (PO_4^{3-} ions were omitted from the map calculation). Distances are indicated in Å. (*a*) PhoA. Ts1 residues that coordinate PhoA are shown in blue. The structurally equivalent residues of Bj-xtrIT are represented in yellow and labelled with their single-letter code. (*b*) PhoB. Lys12 and Trp54 adopt double conformations as indicated by the dark and light blue stick bonds. Arg18^j shown in the figure belongs to a symmetry-related molecule ($j = x + 1, y, z$). Maps are contoured at 1.3σ and were drawn using the program *BOBSCRIPT* (Esnouf, 1997). O atoms are depicted in red, C atoms in grey, N atoms in blue and P atoms in yellow.

during the structural refinement of the Ts1-AR model, two phosphate ions, named PhoA and PhoB, were found to be bonded to the Ts1 molecule (Fig. 2).

3.3.1. PhoA. The refined occupancy for PhoA is equal to 0.92. PhoA is located at the interface between two symmetry-related Ts1 molecules and had already been identified during the Ts1-HR model refinement. PhoA is trapped in a positively charged environment (Fig. 3*a*) formed by N atoms from Lys1, Gly21^{l} and Cys37^{l}, a terminal O atom from Asn49 and a hydroxyl group in one of the conformers of Ser20^{l} from the symmetry-related molecule ($l = 1 - x, y - 1/2, 1 - z$). The average U_{iso} for atoms of the PhoA group is 17 (4) Å^2.

3.3.2. PhoB. The PhoB ion was newly identified during the present atomic resolution structure refinement. It is coordinated by the N atoms of Arg56 (NE and NH2), Lys12 (NZ), and Trp54 (NE1) and four water molecules (Fig. 3*b*). A restrained refinement of the occupational parameter of the Lys12 and Trp54 side chains and of the PhoB ion group converged to 0.60. This indicates that the double conformation of the side chains of residues Lys12 and Trp54 is directly correlated to the presence of PhoB. Fig. 2 shows only the Lys12 and Trp54 side-chain conformations interacting with the phosphate ion. The average U_{iso} for the atoms of Lys12, Trp54 and the PhoB group are 18 (3), 15 (2) and 40 (6) Å^2, respectively. The orientation of PhoB is not well defined and this justifies the high observed U_{iso}. The double conformation of residues Lys12 and Trp54 could be understood by taking into consideration a partial occupancy of the phosphate ions bound to the Ts1 molecule. Thus, the Lys12 and Trp54 side-chain conformations represented by dark and light grey sticks in Fig. 3(*b*) would describe the structure of the Ts1 molecules in the presence and absence of bound phosphate ions, respectively. The PhoB ion does not seem to form strong crystalline contacts: the closest residue from a symmetry-related molecule is Arg18^{j} ($j = x + 1, y, z$), 3.26 (9) Å away from one of the PhoB O atoms (Fig. 3*b*).

3.4. N- and C-termini

In the present Ts1-AR model, the main chain and side chains of Lys1 were found to make different kinds of interactions. The N atom of Lys1 is bound simultaneously to the carbonyl O atom of Leu47 and Asn49, the O3 atom of PhoA and water W48. The NZ atom of the Lys1 side chain interacts with the carboxyl O atom of Val51 and two water molecules, W38 and W81^{k} ($k = 1 - x, y - 1/2, -z$). In fact, W38 and W81^{k} make bridges linking the NZ of Lys1 to the Arg56^{k} and Asn59^{k} side chains, respectively. Thus, the Ts1 N-terminal residue seems to be involved both in crystalline contacts and in anchoring the C-terminus *via* bonds with residues Val51 and Asn4 and with the highly conserved Leu47. Considering that the Ts1 three-dimensional scaffold is firmly maintained by the four disulfide bridges, any chemical modification to its N-terminal residues would reflect directly on the position of its C-terminus.

3.5. Quality of the model

Inspection of the standard deviations (e.s.d.s) of the refined parameters, the distribution of the torsion angles and the peptide planarity of the refined structure all validate the intrinsic quality of the protein structure refinement.

Fig. 4 shows the calculated average e.s.d.s for the atomic coordinates of the main and side chains of Ts1-AR after refinement. The absolute average e.s.d.s for the coordinates of main-chain and side-chain atoms (straight lines in Fig. 4) are 0.04 and 0.08 Å, respectively. As expected, the main-chain e.s.d.s of the atomic coordinates are smaller than average in the strands and in the helical regions and systematically larger than average in the loop region between residues Ser14 and Ser20. All residues with abnormally high e.s.d.s indicated in Fig. 4 point outside the neurotoxin core and, with the exception of Ile17, are charged or polar. Residues Glu2, Tyr45, Trp54 and Asn59 adopt multiple conformation; this justifies their high observed e.s.d.s. Residues Glu9 and Lys31 as well as Asn49 and Asn59 make crystalline contacts with the symmetry-related Ts1 molecules. The side chains of residues Lys52, Arg25 and Lys30 are fully exposed to solvent. All our attempts to refine disordered side chains for residues Ile17 and Lys30 have failed.

The results of *PROCHECK* (Laskowski *et al.*, 1993) indicate that all protein residues of the Ts1-AR structure are located in the most favourable or allowed regions of the Ramachandran plot (Fig. 4). All stereochemical parameters are within the expected limits for this resolution. The overall measure of the stereochemical quality of the model calculated using *PROCHECK* is −0.1 (typical values are between −0.3 and 0.3). In the Ts1-AR model Lys31 has been found in an allowed conformation, whereas in the Ts1-HR refinement it

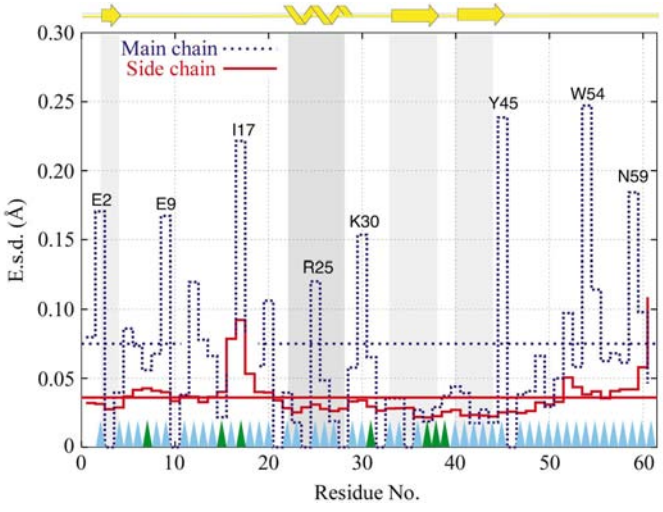

Figure 4
E.s.d.s calculated for main-chain (red lines) and side-chain (blue lines) atoms. Straight lines indicate average values. Residues Glu2, Tyr45, Trp54 and Asp59 are modelled in double conformations; residues Glu9 and Asp59 participate in crystalline contacts; Arg25 and Lys52 are the only residues with no clear electron density for the side chains. Grey areas correspond to α-helices and β-strands. Triangles shown at the bottom of the figure indicate residues located in the most favourable (blue triangles) or allowed (green triangles) regions of the Ramachandran plot.

adopts a generously allowed conformation. The electron density around this residue is extremely well defined and the average e.s.d. and U_{iso} for the Lys31 atoms are 0.03 and 0.25 Å^2, respectively. Pro40 is found in the *cis* conformation, which seems to contribute to the tight bend of the loop between the strands β2 and β3. The final R and R_{free} refinement parameters for the observed [$I \geq 2\sigma(I)$] working-set reflections in the Ts1-AR model are equal to 0.0821 and 0.1391, respectively.

4. Discussion

4.1. Comparison between the Ts1-AR and Ts1-HR models

From both numerical and geometrical points of view, the Ts1-AR refinement can be considered to be more accurate than the Ts1-HR refinement. The major differences between the Ts1-AR and the Ts1-HR models are in the C-terminal and loop regions and in the number of water and phosphate ion molecules bound to the neurotoxin structure. The high reflection per parameter ratio at atomic resolution allowed the refinement of the anisotropic displacement parameters. This procedure reduced the noise level in the maps, permitting the recognition of disordered side chains, new water molecules and a phosphate ion. The overall average r.m.s.d. for all atoms between Ts1-AR and Ts1-HR is 1.4 Å. The most relevant differences between the backbone-atom positions are located in the C-terminal region between residues Ala57 and Cys61 (r.m.s.d. $\simeq$ 2.2 Å). In fact, the C-terminal region has been completely rebuilt. Loops between residues Asp7–Lys12 and Asn48–Val53 also have high r.m.s.d.s. The side chain of Arg56 shows the highest r.m.s.d. ($\sim$6.0 Å) between the models. A careful analysis of the Ts1-HR model has indicated that the Arg56 side chain had been erroneously placed over the position of the second phosphate ion (PhoB) found in the Ts1-AR refinement. Fig. 5 shows the average r.m.s.d. per residue calculated between the Ts1-AR and Ts1-HR models. Significantly misplaced side chains in the Ts1-HR model are also indicated in Fig. 5.

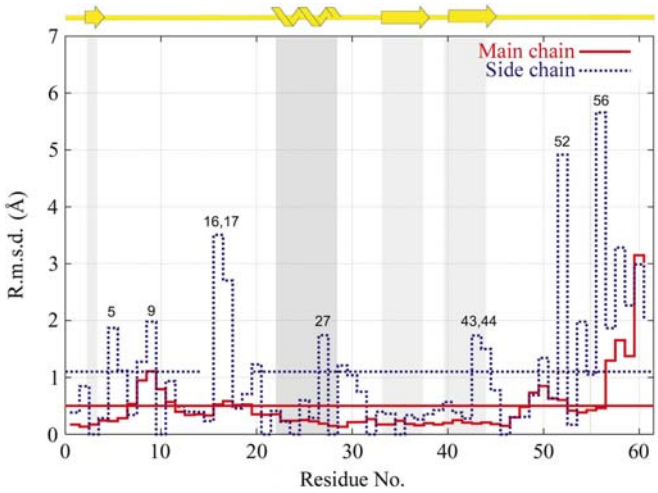

Figure 5
R.m.s. deviations between Ts1-AR (1.16 Å resolution) and Ts1-HR (1.7 Å resolution) models. The red and the blue lines correspond to the r.m.s. deviations between the main chains and side chains of residues, respectively. Straight lines indicate the overall average values. Starting from the residue 55, the main chain was completely reconstructed in the Ts1-AR model compared with the Ts1-HR model. Grey areas correspond to α-helices and β-strands. R.m.s.d.s were calculated using the program *RMS* (Collaborative Computational Project, Number 4, 1994).

4.2. Comparative analysis of Ts1 and other neurotoxins

Ts1 (Polikarpov *et al.*, 1999) and Cn2 (Pintar *et al.*, 1999) are the only β-toxins with known structures, while Bj-xtrIT (Oren *et al.*, 1998) is to date the only excitatory scorpion neurotoxin for which the three-dimensional structure has been determined. So far, no depressant toxin three-dimensional structure has been reported. Ts1 is a classical β-toxin that competes with the depressant insect-specific LqhIT2 and with the excitatory insect-specific AaHIT toxins, binding to closely correlated but distinct receptor sites of the sodium channel (Oren *et al.*, 1998; de Lima *et al.*, 1986; Gordon *et al.*, 1992; Froy *et al.*, 1998; Zilberberg *et al.*, 1997; Barhanin *et al.*, 1984). The origin of the binding competition and the similar pharmacological properties shown by these proteins can be inferred from analysis of the primary sequence and spatial arrangement of residues considered relevant to these protein activities.

4.2.1. The amino-acid sequence. The percentage of invariant and similar residues among the classical α-toxins (those which compete with AaHII and are active in mammals), β-toxins (that compete with CssII and are active in mammals), β-depressant insect-specific (D) and β-excitatory insect-specific (E) scorpion neurotoxins is approximately 20%. All these proteins share the disulfide bridges Cys15–Cys37, Cys23–Cys42 and Cys27–Cys44, the strictly conserved sequences Gly35–Tyr/Trp36–Cys37 and Cys42–Tyr/Trp43–Cys44, the strictly conserved residues Gly3 and Tyr4, Leu/Val47 and an acid (Glu/Asp) residue at position 49 (Fig. 1). The depressant toxin Cn10, active in both insects and crustaceans, has also been considered in the alignment shown in Fig. 1.

Cys11, responsible for anchoring the C-terminus to the CS$\alpha\beta$ motif in classical β-toxins, is not conserved in the E-toxins. Positions 59 in α-toxins and 58 in the primary structure of β-toxins are occupied by positively charged residues which are similarly positioned in their three-dimensional structures. α-, β- and E-toxins possess a pair of basic/acidic residues (Lys/Arg)1-(Glu/Asp/Asn)2 preceding the conserved pair Gly3-Tyr4 at the N-terminus.

Gly10 and Glu26 are invariant among all β-, D- and E-toxin primary sequences. In fact, Glu26 is in the middle of a positively charged area and fully exposed to the solvent in the three-dimensional structures of β-toxins. All β- and D-toxins posses the strictly conserved triad Gly10-Cys11-Lys12, the conserved Lys/Arg25 and aromatic residues Tyr/Trp54.

The amino-acid sequences of the depressant toxin LqhIT2 and Ts1 share 52% similarity. Lys12, Trp39 and Trp54 are among the strictly conserved residues (Fig. 1). In contrast to an apparent characteristic of classical β-toxins, D-toxins do not have a basic residue at their N-terminus. The amino-acid

sequences of the excitatory toxin HaHIT and Ts1 share 45% similarity. There are no aromatic residues at positions 39/40 and 54 of the amino-acid sequence of E-toxins. E-toxins have two basic residues at their N-termini, enhancing the positive potential of this part of the protein. Further similar residues among Ts1, D- and E-toxins are indicated in Fig. 1.

4.2.2. Three-dimensional structures. Fig. 6(*a*) shows a superposition of the backbones of the scorpion β-toxin Ts1, α-toxin AaHII, the E-toxin Bj-xrtrIT and the non-toxic toxin CsE-V3. The overall triangular shape of all these neurotoxins is similar despite the differences in conformation of their C-termini (region IV). An important structural difference between the three-dimensional packings of the toxins lies in the loop region III. In β- and E-toxins this loop is five residues shorter than in α-toxins. As exemplified by AaHII in Fig. 6(*a*), the additional residues in α-toxins extend over residues Gly10-Cys11-Lys12, which are strictly conserved in classical β-toxins (Fig. 1). The short loop in region II and the additional α-helix at the C-terminus distinguish the E-toxin Bj-xrtrIT from the other neurotoxins.

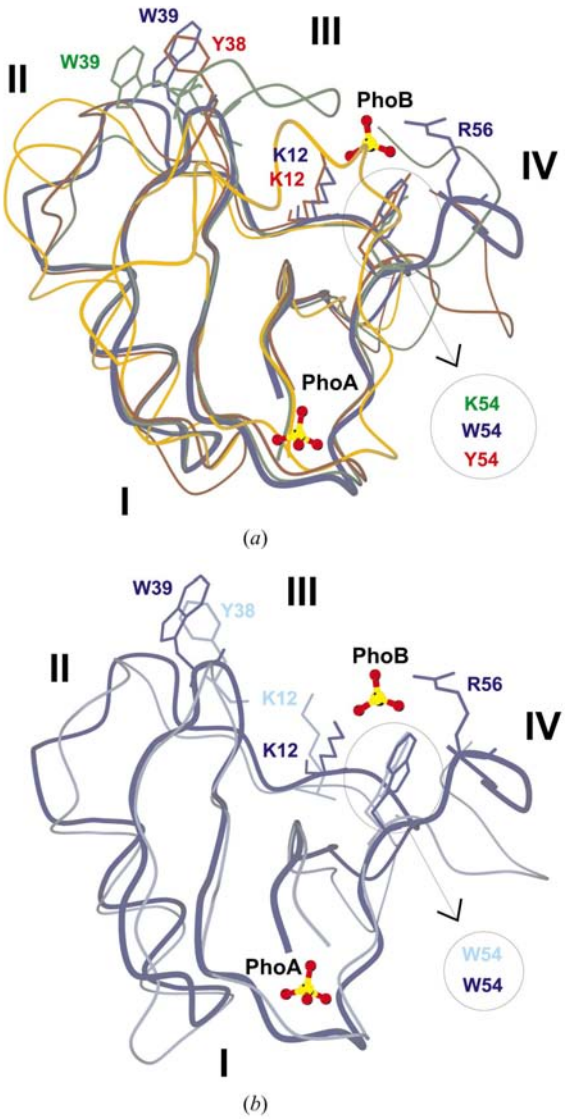

Figure 6
The phosphate ions shown here indicate the Ts1 putative binding sites; however, the Lys12 and Trp54 residues are in the non-bonding conformation (see Fig. 3*b*), allowing a direct comparison between the structures. (*a*) Comparison between the backbones of the classical β-neurotoxin Ts1 (blue), the non-toxic neurotoxin CsE-V3 (red), the α-neurotoxin AaHII (green) and the excitatory toxin Bj-xrtrIT (yellow). (*b*) Comparison between β-neurotoxins Ts1 (blue) and Cn2 (grey), which are both active in mammals. Roman numerals indicate the region with the largest positional differences. Superposition of the structures was performed with the program *COMPARE* (Collaborative Computational Project, Number 4, 1994) and the figures were generated using the program *MOLSCRIPT* (Kraulis, 1991).

Ts1 and Cn2 (Pintar *et al.*, 1999), another scorpion β-neurotoxin active in mammals, share 56% similarity in their primary structure (27 invariant and ten similar residues). The major differences between the three-dimensional structures of the Ts1 and Cn2 neurotoxins lie in the conformation of residues 15–20 (loop I), residues 29–31 (loop II) and residues 55–61 of the C-terminus (region IV) (Fig. 6*b*). Interestingly, the hydrophobic loop I in the Ts1 molecule is shorter than in all other β-toxins and has the same length as an analogous loop in the α-toxins. Nevertheless, its orientation is significantly different from that found in the α-toxins. Loop II in most of the β-toxins is two residues longer than in α-toxins (Fig. 1). Ts1 is an exception among the β-toxins in this respect. Remarkably, its loop II has the same length and the same spatial orientation as the corresponding loop of the α-toxins (Fig. 6*a*).

4.3. β-Toxin binding competition

4.3.1. Ts1 competition with depressant toxins. The aromatic residue Trp/Tyr54 is conserved in all β- and D-toxins (Fig. 1). The position and orientation of this aromatic residue, shown in Fig. 6(*b*), does not change significantly among the Ts1 and Cn2 structures. Thus, both the aromatic character of the residue and its orientation in the three-dimensional structure seem to be characteristic of classical β-toxins. In general, there is an aromatic residue at position 39 in the α-toxins and at position 40 in the primary structures of β- and D-toxins (Fig. 1). Ts1, with the tryptophan residue at position 39 of its amino-acid sequence, is the only exception among the β-toxins. Fig. 6(*a*) shows that all these aromatic residues are in the loop region III, between the strands β2 and β3, occupying the same region in all the refined three-dimensional structures.

Lys12 is strictly conserved in all classical β- and D-toxins (Darbon *et al.*, 1983). Its side chain has the same orientation in the Ts1 and CsE-V3 refined models. Note that the samples used in both of these studies were crystallized at physiological pH. Some of the Lys12 side chains in the conformers of the non-toxic CsE-V1 and CsE-I and from the β Cn2 NMR structures also have a similar orientation to that encountered in the Ts1 structure (Fig. 6*b*). Analysis of the three-dimensional structures of the α-toxins shows that a positively charged residue Arg/Lys54 occupies the same space as Trp/Tyr54 in β-toxins (Fig. 6*a*). Therefore, a basic residue Arg/Lys54 in α-toxins and Lys12 in β-toxins could play the same binding or recognition role. Lys11 in the excitatory toxins aligns with Lys12 in β- and D-neurotoxins, but has a

completely different neighbourhood in the three-dimensional structure of the excitatory toxin Bj-xrtrIT.

In Ts1, the side chains of the residues Lys12, Trp54 and Arg56 (Fig. 2) coordinate the PhoB ion. Note that the Ts1 polypeptide main-chain conformation at the C-terminus seems to contribute to the positioning of the Arg56 side chain (Figs. 6*a* and 6*b*). Arg56 is not conserved in the β-toxins. However, owing to its position in the three-dimensional structure, it clearly enhances both the size and intensity of the area of positive potential near the PhoB-binding site (Fig. 7). The shape and the position of the cavity formed by residues Lys12–Trp54 seem to be conserved among the β scorpion long-chain toxins (Figs. 6*a* and 6*b*). Despite the observed double conformation of the side chains of Trp54 and Lys12, the general feature of the Lys12–Trp54 cavity is preserved in the Ts1.

Toxicity tests performed in mice and binding-affinity tests in rat brain and cockroach nerve cord have shown that residues Trp54 and Trp39 from the aromatic conserved cluster and the positively charged residue Lys12 are important for Ts1 activity (Hassani *et al.*, 1999). From the structural properties discussed above and from the sequence alignment, it is likely that aromatic residues at positions 39/40 are crucial for the binding of both α- and β-toxins to the recognition site of the Na^+ channel. Tyr/Trp54 and Lys12 seem to be involved in the binding specificity of the classical β-toxins.

Therefore, a plausible explanation for the binding competition between Ts1 and LqhIT2 (*i.e.* Ts1 and D-toxins) is that in addition to similarities in primary and tertiary structures, both have conserved the Lys12–Trp54 binding cavity.

4.3.2. Ts1 competition with excitatory toxins. Crystallographic studies and site-directed mutagenesis experiments performed on the excitatory toxin Bj-xtrIT allowed identification of the putative bioactive surface of this insect-selective neurotoxin isolated from the scorpion *Buthotus judaicus* (Froy *et al.*, 1998; Oren *et al.*, 1998; Zilberberg *et al.*, 1997; Gurevitz *et al.*, 2001). The bioactive surface is composed mainly of the amino-acid residues of the N- and C-termini, comprising Lys1, Lys2, Asn28, Thr32, Lys33, Tyr36, Ala37, Asp54, Asp55, Lys56, Asp70, Ile73 and Ile74 (Bj-xtrIT numbering; Froy *et al.*, 1998). Mutagenesis and biochemical modifications of the residues composing this surface result in inactive or poorly active toxins (Froy *et al.*, 1998; Oren *et al.*, 1998; Possani *et al.*, 1985; el Ayeb *et al.*, 1986; Kharrat *et al.*, 1990). Lys1 and Asn49 of the Ts1 molecule, coordinating the phosphate ion PhoA, are the equivalents of Lys2 and Asp54 in Bj-xtrIT, being spatially located right at the middle of the putative bioactive surface of the excitatory toxins (Fig. 3*a*). The PhoA-binding site might therefore represent a footprint of the sodium-channel receptor-binding site on both Ts1 and excitatory toxins, explaining the reason for their competition for Na^+ channels. Scission of the N- or C-termini, as well as biochemical modifications and mutations of the residues in the putative bioactive surface area, perturb the PhoA-binding site, leading to significant decrease of both Ts1 and E-toxin sodium-channel binding affinity.

4.3.3. Ts1 binding sites in Na^+ channels. Structural evidence for the existence of at least two sodium-channel binding sites in the Ts1 neurotoxin deserves additional discussion. It is known that α-toxins bind to a cluster of homologous but not identical receptor-binding sites on both rat brain and insect sodium channels (Gordon *et al.*, 1996). β-Toxins have been shown to bind to two classes of specific high-affinity sites on purified sodium channels (Thomsen *et al.*, 1995). Furthermore, the depressant toxins have been shown to posses two non-interacting binding sites on the insect sodium channel: a high-affinity and a low-affinity site (Gordon *et al.*, 1992; Cestèle *et al.*, 1997; Cestèle & Catterall, 2000). Excitatory toxins, on the other hand, bind to a single class of receptor sites and compete with depressant toxins only for the high-affinity binding site (Gordon *et al.*, 1992; Cestèle *et al.*, 1997; Cestèle & Catterall, 2000). The antibody-mediated inhibition of the excitatory and depressant toxins binding suggests that their sodium-channel binding sites are localized in close

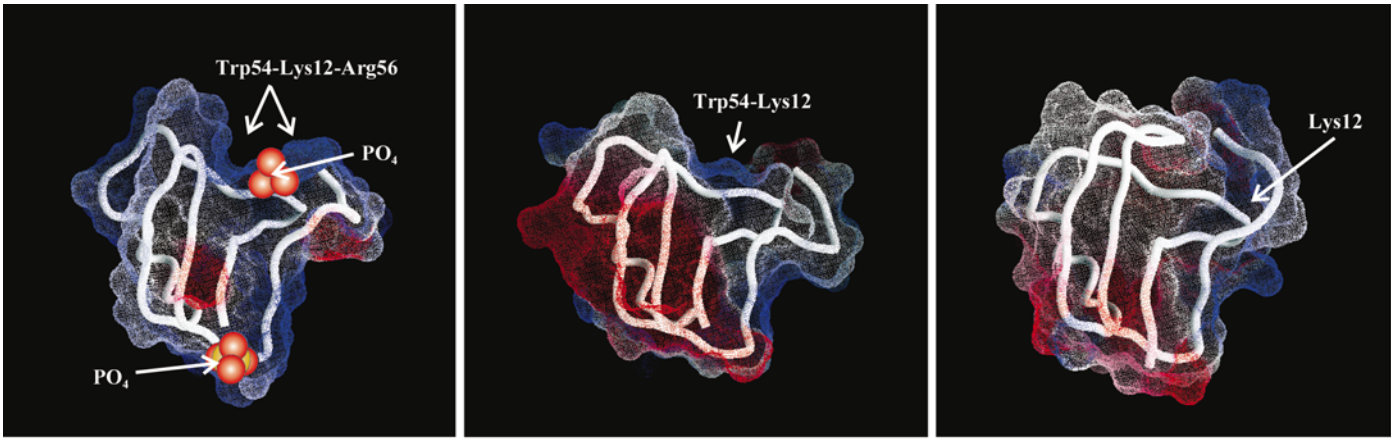

Figure 7
Distribution of electrostatic charge at the surface of Ts1 and CsE-V3 β-toxins and AaHII α-toxin as calculated by *GRASP* (Nicholls *et al.*, 1991). Blue and red indicate positive and negative potential regions, respectively. The proteins are shown in the same orientation and with the same charge-distribution scale. Protein backbones and positions of functionally important residues are also indicated.

proximity but are not identical, in spite of the competitive inhibition between these toxins (Gordon *et al.*, 1992). Moreover, the β-toxin Ts1, which possesses a high affinity for receptor site 4 (Gordon *et al.*, 1992) on both mammal and insect sodium channels, competitively inhibits the binding of excitatory toxins as well as depressant toxins.

In view of these observations, it is not surprising that Ts1 specifically and neurotoxins in general could have more then one sodium-channel binding site. Indeed, it is highly improbable that the complexity of the interactions of the neurotoxins with the Na^+ channels and the binding competition between different types of toxins could be attributed to a single binding site. Structural evidence for the existence of at least two sodium-channel binding sites mapping to the phosphate ions in the Ts1 structure provides a good starting point for further site-directed mutagenesis, competition binding and electrophysiological experiments.

5. Conclusion

In the present work, we have determined the structure of the highly toxic scorpion β-neurotoxin Ts1 (Ts-γ or Ts VII) at atomic resolution and compared it with the available three-dimensional models of neurotoxins of different classes. The differences in three-dimensional structure and amino-acid sequence between classical α- and β-, E- and D-toxins are described in detail and structural properties putatively correlated with the competition between excitatory, depressant and Ts1 toxins for sodium-channel binding sites are discussed.

No non-proline *cis*-peptide bonds has been observed in Ts1-AR, in contrast to the BmK M1 and BmK M4 structures (He *et al.*, 1999). In addition, contrary to a number of atomic resolution X-ray structures and NMR models (Zhao *et al.*, 1992; Housset *et al.*, 1994; Landon *et al.*, 1996), all four existing disulfide bonds have been found in a single conformation. Although several basic residues are exposed to the solvent on the Ts1 protein surface, only the Lys1, Lys12 and Arg56 side chains interact with the phosphate ions present in the crystallization solution. The two phosphate ions found in the 1.16 Å resolution electron-density map most probably correspond to Na^+-channel binding sites on the protein.

One of the phosphate ions is bound to the N-terminal basic residue of Ts1 (Lys1), which from chemical modification and site-directed mutagenesis studies has been considered to be important for the high toxicity displayed by this toxin. In addition, the C-terminus is located in the direct vicinity of the N-terminus, forming together with the N-terminal residues a putative bioactive area of these proteins. It is tempting to suggest that PhoA pinpoints the possible sodium-channel binding site used by both Ts1 and excitatory neurotoxins. As a consequence, these neurotoxins compete with each other in receptor binding.

The second phosphate ion induces a conformational change of the Lys12–Trp54–Arg56 cavity, which in the Ts1 structure has the largest positively charged surface area of any α- or β-toxins studied structurally to date. The cavity formed by the residues Lys12–Tyr54/Trp54 seems to be conserved in all classical β-toxins and is stereochemically required for interaction with the sodium channel. The presence of the bound phosphate ion in the Ts1 toxin Arg56–Lys12–Trp54 cavity, the binding affinity and the degree of toxicity correlated with residues Lys12/Trp54 all further strengthen the importance of this binding/toxic site in Ts1. Finally, the existence of the Lys12–Tyr54 cavity seems to be a structural reason for competition between Ts1 and the depressant LqhIT2 toxin in binding to insect nerve-cord synaptosomal preparations.

The putative sodium-channel binding sites in the Ts1 neurotoxin are distinct in terms of their stereochemical arrangement and location in the structure; however, they interact with the same ligand, the phosphate ion. This fact strongly suggests that Ts1 in particular and neurotoxins in general can specifically interact with negatively charged binding sites on the Na^+ channel, modifying its physiological properties and competing with each other in binding.

This work was supported by the FAPESP (Fundação de Amparo à Pesquisa do Estado de São Paulo) grants 99/08042-5 and 99/03387-4. We thank Professor Oussama Hassani for kindly providing us with the coordinates of the Ts1 neurotoxin obtained by comparative modelling and the LNLS personnel for giving us access to the synchrotron-facility infrastructure.

References

Ayeb, M. el, Darbon, H., Bahraoui, E. M., Vargas, O. & Rochat, N. (1986). *Eur. J. Biochem.* **155**, 289–294.
Barhanin, J., Giglio, J. R., Leopold, P., Schimid, A., Sampaio, S. V. & Lazdunski, M. (1982). *J. Biol. Chem.* **257**, 12553–12558.
Barhanin, J., Ildefonse, M., Rougier, O., Sampaio, S. V. Giglio, J. R.& Lazdunski, M. (1984). *Pflügers Arch.* **400**, 22–27.
Blanc, E., Hassani, U., Meunier, S., Mansuelle, P., Sampieri, F., Rochat, H. & Darbon, H. (1997). *Eur. J. Biochem.* **247**, 1181–1126.
Brünger, A. T. (1992). *Nature (London)*, **355**, 472–475.
Brünger, A. T., Adams, P. D., Clore, G. M., DeLano, W. L., Gros, P., Grosse-Kunstleve, R. W., Jiang, J. S., Kuszewski, J., Nilges, M., Pannu, N. S., Read, R. J., Rice, L. M., Simonson, T. & Warren, G. L. (1998). *Acta Cryst.* D**54**, 905–921.
Burley, S. K. & Petsko, G. A (1985). *Science*, **229**, 23–28.
Catterall, W. A. (1992). *Physiol. Rev.* **72**, S15–S48.
Cestèle, S. & Catterall, W. A. (2000). *Biochimie*, **82**, 883–892.
Cestèle, S., Kopeyan, C., Oughideni, R., Mansuelle, P., Granier, C. & Rochat, H. (1997). *Eur. J. Biochem.* **243**, 93–98.
Collaborative Computational Project, Number 4 (1994). *Acta Cryst.* D**50**, 760–763.
Couraud, F., Jover, E., Dubois, J. M. & Rochat, H. (1982). *Toxicon*, **20**, 9–16.
Darbon, H., Jover, E., Couraud, F. & Rochat, H. (1983). *Int. J. Pept. Protein Res.* **22**, 179–186.
Esnouf, R. M. (1997). *J. Mol. Graph. Model.* **15**, 132–134.
Fontecilla-Camps, J. C., Almassy, R. J., Suddath, F. L. & Bugg, C. E. (1981). *Trends. Biochem. Sci.* **6**, 291–296.
Froy, O., Zilberberg, N., Gordon, D., Turkov, M., Gilles, N., Stankiewicz, M., Pelhate, M., Loret, E., Oren, D. A., Shaanan, B. & Gurevitz, M. (1998). *J. Biol. Chem.* **274**, 5769–5776.
Golubev, A. M., Lee, W. H., Marangoni, S., Novello, J. C., Oliveira, B., Toyama, M. H. & Polikarpov, I. (1998). *Acta Cryst.* D**54**, 1440–1441.

Gordon, D., Martin-Euclaire, M. F., Celeste, S., Kopeyan, C., Carlier, E., Ben Khalifa, R., Pelhate, M. & Rochat, H. (1996). *J. Biol. Chem.* **271**, 8034–8045.
Gordon, D., Moskowitz, H., Eitan, M., Warner, C., Catterall, W. A. & Zlotkin, E. (1992). *Biochemistry*, **31**, 7622–7628.
Gordon, D., Savarin, P., Gurevitz, M. & Zinn-Justin, S. (1998). *J. Toxicol. Toxin Rev.* **17**, 131–159.
Gurevitz, M., Gordon, D., Ben-Natan, S., Turkov, M. & Froy, O. (2001). *FASEB J.* **15**, 1201–1205.
Hassani, O., Mansuelle, P., Cestèle, S., Bourdeaux, M., Rochat, H. & Sampieri, F. (1999). *Eur. J. Biochem.* **260**, 76–86.
He, X. L., Deng, J. P., Wang, M., Zhang, Y. & Wang, D. C. (2000). *Acta Cryst.* D**56**, 25–33.
He, X. L., Li, H. M., Zeng, Z. H., Liu, X. Q., Wang, M. & Wang, D. C. (1999). *J. Mol. Biol.* **292**, 125–135.
Housset, D., Habersetzer-Rochat, C., Astier, J. P. & Fontecilla-Camps, J. C. (1994). *J. Mol. Biol.* **238**, 88–103.
Jablonsky, M. J., Jackson, P. L., Trent, J. O., Watt, D. D. & Krishna, N. R. (1999). *Biophys. Res. Commun.* **254**, 406–412.
Jablonsky, M. J., Watt, D. D. & Krishna, N. R. (1995). *J. Mol. Biol.* **248**, 449–458.
Johnson, C. K. (1970). *Crystallographic Computing*, edited by F. R. Ahmed, pp. 220–226. Copenhagen, Denmark: Munksgaard.
Jones, T. A., Zou, J. Y., Cowan, S. W. & Kjeldgaard, M. (1991). *Acta Cryst.* A**47**, 110–119.
Jover, E., Couraud, F. & Rochat, H. (1980). *Biochem. Biophys. Res. Commun.* **95**, 1607–1614.
Jover, E., Moutot-Martin, N., Couraud, F. & Rochat, H. (1980). *Biochemistry*, **19**, 463–467.
Kharrat, R., Darbon, H., Granier, C. & Rochat, H. (1990). *Toxicon*, **28**, 509–523.
Kharrat, R., Darbon, H., Rochat, H. & Granier, C. (1989). *Eur. J. Biochem.* **181**, 381–390.
Konnert, J. H. & Hendrickson, W. A. (1980). *Acta Cryst.* A**36**, 344–350.
Kraulis, P. (1991). *J. Appl. Cryst.* **24**, 946–950.
Krimm, I., Gilles, N., Sautiere, P., Stankiewicz, M., Pelhate, M., Gordon, D. & Lancelin, J. M. (1999). *J. Mol. Biol.* **285**, 1749–1763.
Landon, C., Cornet, B., Bonmatin, J. M., Kopeyan, C., Rochat, H., Vovelle, F. & Ptak, M. (1996). *Eur. J. Biochem.* **236**, 395–404.
Landon, C., Sodano, P., Cornet, B., Bonmatin, J. M., Kopeyan C., Rochat, H., Vovelle, F. & Ptak, M. (1997). *Proteins*, **28**(3), 360–374.
Laskowski, R. A., MacArthur, M. W., Moss, D. S. & Thornton, J. M. (1993). *J. Appl. Cryst.* **26**, 283–291.
Lee, W., Jablonsky, M. J., Watt, D. D. & Krishna, N. R. (1994). *Biochemistry*, **33**, 2468–2475.
Li, H. M., Wang, D. C., Zeng, Z. H., Jin, L. & Hu, R. Q. (1996). *J. Mol. Biol.* **261**, 415–431.
Lima, M. E. de & Martin-Euclaire, M. F. (1995). *J. Toxicol. Toxin Rev.* **14**, 457–481.
Lima, M. E. de, Martin-Euclaire, M. F., Diniz, C. R. & Rochat, H. (1986). *Biochem. Biophys. Res. Commun.* **139**, 296–302.
Meves, H., Simard, M. & Watt, D. D. (1984). *Ann. NY Acad. Sci.* **79**, 185–191.
Moews, P. C. & Kretsinger, R. H. (1975). *J. Mol. Biol.* **91**, 201–225.
Nicholls, A., Sharp, K. A. & Honig, B. (1991). *Proteins Struct. Funct. Genet.* **11**, 281–296.
Oren, D. A., Froy, O., Amit, E., Kleinberger-Doron, N., Gurevitz, M. & Shaanan, B. (1998). *Structure*, **9**, 1095–1103.
Otwinowski, Z. & Minor, W. (1993). *DENZO. A Film Processing Program for Macromolecular Crystallography*. Yale University, New Haven, CT, USA.
Pelhate, M. & Zlotkin, E. (1982). *J. Exp. Biol.* **97**, 67–77.
Pintar, A., Possani, A. M. & Delepierre, M. (1999). *J. Mol. Biol.* **287**, 359–367.
Polikarpov, I., Oliva, G., Castellano, E. E., Garratt, R. C., Arruda, P., Leite, A. & Craievich, A. (1998). *Nucl. Instrum. Methods A*, **405**, 159–164.
Polikarpov, I., Perles, L. A., de Oliveira, R. T., Oliva, G., Castellano, E. E., Garratt, R. C. & Craievich, A. (1998). *J. Synchrotron Rad.* **5**, 72–76.
Polikarpov, I., Sanches, M. S. Jr, Marangoni, S., Toyama, M. H. & Teplyakov, A. (1999). *J. Mol. Biol.* **290**, 175–184.
Possani, L. D., Becerril, B., Delepierre, M. & Tytgat, J. (1999). *Eur. J. Biochem.* **264**, 287–300.
Possani, L. D., Martin, B. M., Mochca-Morales, J. & Svendsen, I. (1981). *Carlsberg Res. Commun.* **46**, 195–205.
Possani, L. D., Martin, B. M., Svendsen, I., Rode, G. S. & Erickson, B. W. (1985). *Biochem. J.* **229**, 739–750.
Selisko, B., Garcia, C., Becerril, B., Delepierre, M. & Possani, L. D. (1996). *Eur. J. Biochem.* **242**, 235–242.
Sheldrick, G. M. & Schneider, T. R. (1997). *Methods Enzymol.* **277**, 319–343.
Thompson, J. D., Higgins, D. G. & Gibson, T. J. (1994). *Nucleic Acids Res.* **22**, 4673–4680.
Thomsen, W., Martin-Eaclair, M. F., Rochat, H. & Catterall, W. A. (1995). *J. Neurochem.* **65**, 1358–1364.
Tugarinov, V., Kustanovich, I., Zilberberg, N., Gurevitz, M. & Anglister, J. (1997). *Biochemistry*, **36**, 2414–2424.
Zhao, B., Carson, M., Ealick, M. & Bugg, C. E. (1992). *J. Mol. Biol.* **277**, 239–252.
Zilberberg, N., Froy, O., Loret, E., Celeste, S., Arad, D., Gordon, D. & Gurevitz, M. (1997). *J. Biol. Chem.* **272**, 14810–14816.
Zlotkin, E. (1993). *In Toxins and Signal Transduction*, edited by P. Lazarowici & Y. Gutman, pp. 95–117. Amesterdam: Harwood Press.
Zlotkin, E., Kadouri, D., Gordon, D., Pelhate, M., Martin-Eauclaire, M. F. & Rochat, H. (1985). *Arch. Biochem. Biophys.* **240**, 877–887.
Zlotkin, E., Miranda, F. & Rochat, H. (1978). *Handbook of Experimental Physiology*, Vol. 48, edited by S. Bettini, pp. 317–369. Heidelberg: Springer–Verlag.